Research Article **Open Access**

The Summer Distribution of Dissolved Inorganic Iodine along 18°N in the South China Sea

Long A[1,*], Dang A[1,2], Xiao H[1] and Yu X[1,3]

[1]State Key Laboratory of Tropic Oceanography, South China Sea Institute of Oceanology, Chinese Academy of Sciences, 164 West Xingang Road, Guangzhou 510301, P.R China
[2]South China Sea Branch of the State Oceanic Administration, 353 Middle Xingang Road, Guangzhou, 510301, P.R China
[3]University of Chinese Academy of Sciences, Beijing, 100039, P.R China

Abstract

Dissolved inorganic iodine (iodate and iodide) in seawater samples collected in the northern South China Sea (SCS) were investigated using differential pulse polarography and cathodic stripping square wave voltammetry, respectively. High concentration of iodide was observed in the surface layer in agreement with those previously reported for tropical waters. Iodine speciation and macro-nutrients were strongly coupled as observed in other tropical oceans. The vertical distributions of iodine and macro-nutrients can be classified into three biogeochemical regimes: (1) in the upper 50 m of the water column, low iodate was observed as nutrients were depleted and photosynthesis was low in summer. In contrast, substantial amount of iodide produced by high phytoplankton productivity and intense bacterial action in winter and spring was saved till summer; (2) in the water column between 50 m and the Tropical Water at around 150 m, the amount of iodide oxidation varied proportionally with nitrification, leading to rapid increase of nitrate and iodate with depth; (3) below the Tropical Water, iodate and nitrate are regenerated mainly due to re-mineralization of organic matter sinking from the euphotic zone. The distribution of dissolved inorganic iodine and hydrographic parameters (salinity, temperature, dissolved oxygen, and macro-nutrients) were influenced by the downwelling of the mesoscale warm eddy.

Introduction

There has been interest in the biogeochemical cycling of iodine in recent decades for its own sake and due to the importance of this element in human health, hydrologic processes and radioecology [1]. Compared to low levels of iodine found in soils, rivers, lakes and terrestrial plants, oceans are the major source of iodine in the global geochemical cycle with an average oceanic iodine concentration of approximately 0.45 μM. Although thermodynamic calculation indicates that iodate should be more stable than iodide in oxic seawater [2-4], field studies have observed pronounced conversion of iodate to iodide in permanently stratified surface waters not only in tropical and sub-tropical oceans [5-9], but also in temperate continental shelf seas where iodide concentration increase shoreward [10-14]. Thus, the overall longitudinal distribution of iodate in the surface layer shows that iodate concentration increases polewards whereas iodide concentration maxima is observed near the equator [5,15]; meanwhile, the general vertical trend shows that iodide decreases with depth to around the detection limit below the euphotic zone while iodate increases with depth to an approximately constant level [16]. Furthermore, iodide can be enriched in anoxic basins and oxygen minimum zones.

Understanding the controls on dissolved iodine speciation is important because of its role in the global biogeochemical cycle of iodine and indirect effect on the supply of iodine to the atmosphere from the oceans [17]. Once iodine enters the atmosphere, it can promote particle formation reactions in the marine boundary layer and very effectively destroy ozone, thus influencing climate [18].

In a redox cycle, iodate and iodide are interconverted, and this is the most pronounced effect for iodine speciation in oxic seawater [19]. However, the evidence for the actual mechanisms of iodate reduction to iodide in oxic oceanic waters remains unclear [20-22]and our knowledge on iodide oxidation to iodate has been limited [23], making it difficult to adequately model iodine cycling in the ocean.

The South China Sea (SCS) is the largest marginal sea of the world [24] and is situated in the tropical-subtropical zone where active interconversion between iodate and iodide is expected. The study of iodine in the SCS may provide insight into mechanisms controlling global ocean iodine cycle. However, few data are available on the spatial distribution of iodine in the SCS. In this work, the spatial distribution of dissolved inorganic iodine in the SCS and the implications for the interconversion between iodate and iodide are studied and the implication on the biogeochemical dynamics of the dissolved iodine system in the marginal seas is discussed.

Study area

As a result of a unique combination of environmental conditions, the characteristics of its upper water are significantly different from those in other low-latitude areas and these differences have led to patterns in the intra-seasonal variations in phytoplankton biomass that are atypical of low-latitude waters [25-27].

The SCS is the largest semi-enclosed tropical marginal sea in the northwest Pacific Ocean with a total area of 3.5 million km2 often

referred to as the Asian Mediterranean, e.g., Morton and Blackmore [28]. The maximum depth of the SCS exceeds 5000 m, while its mean depth is 1350 m [24]. Thus, the South China Sea combines characteristics of open oceans and confined marginal seas.

The northern part of the SCS has a broad continental shelf (150-250 km offshore) which has an average depth of shallower than 200 m and has isobaths that are parallel to the continental coastline. Along the northern boundary, the Pearl River Estuary (PRE) is located between the Taiwan Shoal and the Hainan Island. The annual average river discharge through the PRE is 10 524 m3s-1, with 80% occurring between April and September during the period of the summer monsoon. Under the influence of the summer monsoon, the less saline river discharge of over 16,000 m-3 s-1 influences the broad region over the shelf [29]. In addition, the southwesterly summer monsoon can induce upwelling at many places over the continental shelf, which is a seasonal common phenomenon with the spatial extent of a basin-scale in the NSCS [30,31].

In this study, we focused on the 18°N transect including 13 stations stretching from 110°E to 119.5°E (Figure 1). In the west section of this transect stations 1 and 2 are close to the Hainan Island, with depths of 94 m and 156 m respectively. The station 13 locates at about 100 km from the south of Luzon Strait.

Sampling and analyses

Sampling was conducted aboard the R/V "Shiyan 3" during KJ cruise in June 2014. Seawater samples were collected using a conductivity-temperature-depth (CTD) rosette equipped with 12 modified Hydro-Bios 2 L water bottles.

Sub-samples for dissolved oxygen (DO) were measured by the standard manual Winkler's method [32]. Samples for the determination of nutrients were filtered and frozen until analysis within 3 weeks after sample collection. The concentrations of nitrate, nitrite and phosphate were determined by standard methods [32].

Water samples for dissolved inorganic iodine species (iodate and iodide) analysis were collected were filtered and stored frozen in the dark. All samples were analyzed within 2 months. Both iodate and iodide were determined by using Metrohm Model 797 VA Computrace (Switzerland) in conjunction with a hanging mercury drop electrode, a platinum auxiliary electrode and a reference Ag/AgCl/KCl (3

mol/L) electrode. Iodate was determined directly by differential pulse polarography according to the method of Wong and Zhang [33] adapted from protocol of Herring and Liss [34]. Iodide was determined by Cathodic Stripping Square Wave Voltammetry according to the original method of Luther et al. [35]. The analyses were carried out using standard addition with calibration plot method. Three additions were added to the original sample and each was scanned in duplicate. Each sample was measured in duplicate or triplicate. The coefficient of variation was typically less than ± 5% for iodate and ± 9% for iodide. Detection limits of the iodate and iodide analyses were around 20 nM and 5 nM, respectively.
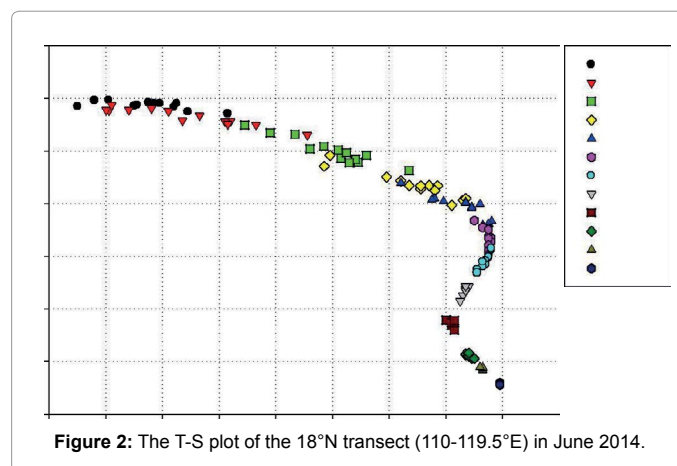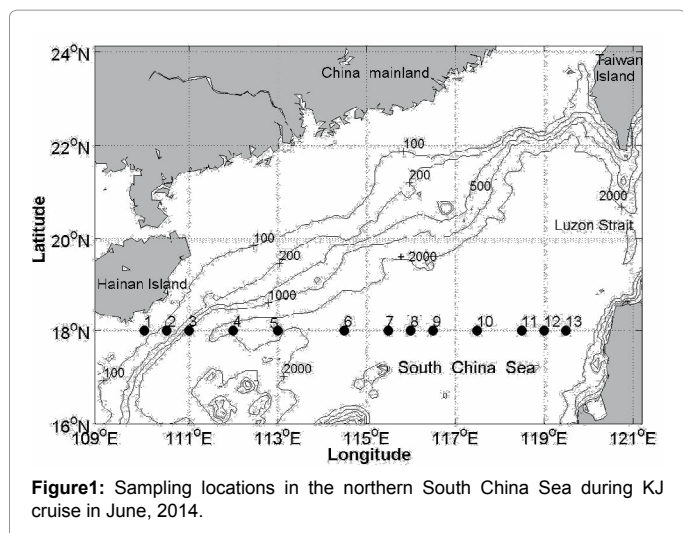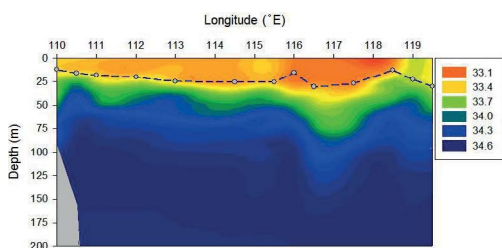
Results

Hydrography

The vertical distributions of salinity and temperature above 1500 m are in accordance with those reported previously in the northern SCS [36]. Salinity increases with depth to a maximum at around 150 m, which represents the Tropical Water. Then it decreases to a minimum at around 500 m, which represents the North Pacific Intermediate Water (NPIW). Below the NPIW, salinity increases slightly from 34.4 to 34.6 at 1500 m. In contrast, temperature decreases linearly with depth, with a strong gradient in the top 200 m layer. The T-S plot (Figure 2) shows that salinity and temperature were uniform below 200 m and variable in the top 200 m as shown in Figure 3.
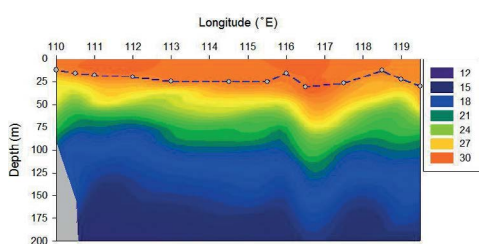
These variations were caused by typical hydrological events of the South China Sea. A mesoscale eddy converging warm waters was progressing between 116°E and 118°E during the sampling period. The downwelling movement of the water within this warm eddy was clearly demonstrated by the depressed isopleths of salinity and temperature. While stations 9 and 10 were located at the center of this eddy, stations 6, 7 and 11, 12 recorded the peripheral vertical convections. On the western side of this latitudinal transect, stations 1 and 2 were located on the continental shelf where upwelling prevails in summer [31]. The upwelling centers of QDU (in the east of the Hainan Island) were located at (19°45'N, 111°10'E) and (18°25'N, 110°15'E), and stations 1 and 2 were close to the latter one. The higher salinity at these two stations, relative to the more offshore water, was attributed to the influence of upwelling at that time.

High insolation causes relatively high sea-surface temperature in the SCS, exceeding 29°C (Figure 3a). Meanwhile, large inputs of fresh water from terrestrial runoffs and precipitation during this season reduced

Figure1: Sampling locations in the northern South China Sea during KJ cruise in June, 2014.

Figure 2: The T-S plot of the 18°N transect (110-119.5°E) in June 2014.
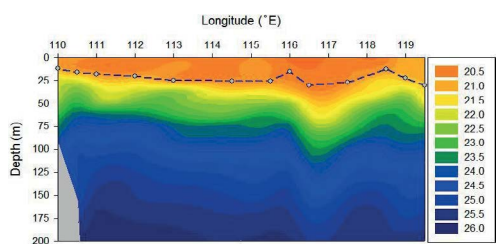
(3b) Temperature.

(3c) Density.

Figure 3: Spatial variations of (3a) salinity, (3b) temperature and (3c) density in the top 200m along the 18°N transect (110-119.5°E) in June 2014. The values of mixed layer depth (MLD) were derived from a drop of 0.5°C from the sea-surface temperature (Karl and Lukas, 1996) and shown with blue short-dash line. The gray circles represent sampling stations. (3a) Salinity.
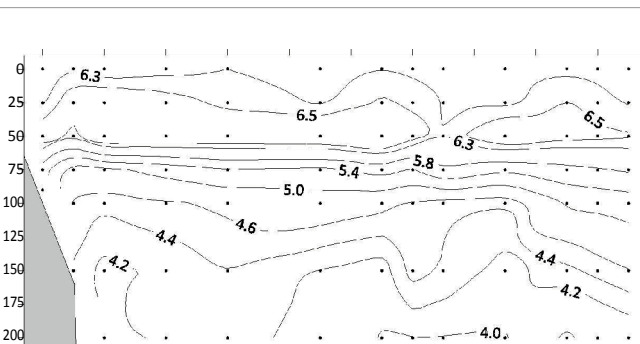

Figure 4: Spatial variations of DO in the top 200m along the 18°N transect (110-119.5°E) in June 2014. The unit is mg O_2/L. Dark dots represent the sampling sites.

the salinity to below 33.7 in the upper 30 m of the water column (Figure 3b). Therefore, the upper layer was stratified and the mixed layer depths (MLD) were less than 30 m along this transect (Figure 3c). This result is consistent with Wong et al. [36], which shows a mixed layer depth of 20 ± 6 m during summer.

Dissolved oxygen (DO)

The vertical distribution of DO above 200 m (Figure 4) exhibits a subsurface maximum between 25 and 50 m, and a rapid decrease with depth below 50 m, in particular between 50 m and 100 m. This DO profile appears to be related to biological activities and re-mineralization.

Nutrients

The vertical distributions of dissolved inorganic nutrients in the upper 1500 m water column and the distributions of these parameters in the top 200 m are shown in Figures 5a and 6. Within the upper 50 m of the water column, nitrate was below detection limit, except the low values (0.1~0.2 μM) at stations 1 and 2 on the continental shelf. The
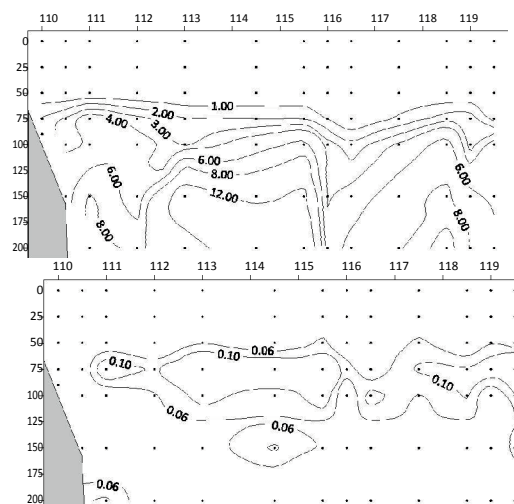
(5c) Phosphate.

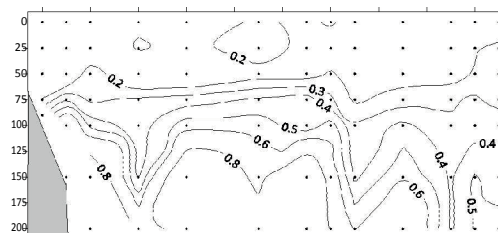

Figure 5: Spatial variations of (5a) nitrate, (5b) nitrite, (5c) phosphate in the top 200m along the 18°N transect (110-119.5°E) in June 2014. Dark dots represent the sampling sites. The unit is μM.(5a) Nitrate. (5b) Nitrite. (5c) Phosphate.
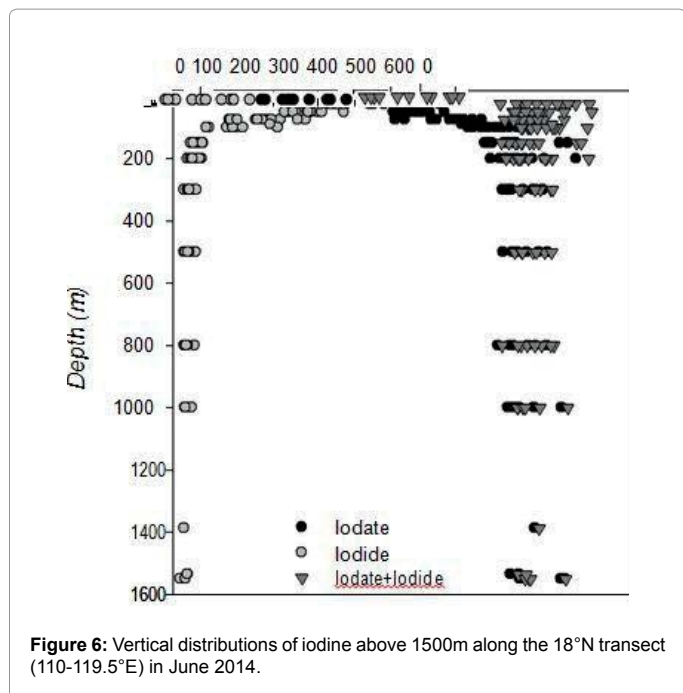
Figure 6: Vertical distributions of iodine above 1500m along the 18°N transect (110-119.5°E) in June 2014.

presence of nitrate there may be due to terrestrial input or upwelling input. Furthermore, phosphate in this water was quite low (~0.1 μM), even undetectable in the warm eddy and on the continental shelf. Below 50 m, both nitrate and phosphate increased with depth (Figure 5b). A strong gradient was observed between 50 m and 500 m probably due to intensive re-mineralization of sinking organic matter. The primary nitrite maximum (>0.1 μM) was located between 50 and 100 m where nitrification was extensive [37,38]. Although the vertical spacing of samples was inadequate to precisely depict and could introduce distortions into the details in the distribution of nitrite in this layer of water, the general feature was clear. Because of the converging and downwelling effect of the warm core eddy, nitrate, nitrite and phosphate isopycnals were apparently depressed, just like those of temperature and salinity.

Dissolved inorganic iodine

The vertical distributions of iodine above 1500 m and the spatial variations of iodate and iodide in the top 200 m layer along this transect were plotted in Figures 5c and 7a,7b. All 13 stations can be grouped into two different patterns according to iodine distribution. At stations 2, 6, 7, 10, 11 and 12, iodine was quite constant in the water column without obvious surface depletion. In contrast, significant iodine surface enrichments were observed in stations 1, 3, 4, 5, 8, 9 and 13. Iodide and iodate concentrations at the surface of these stations were higher than 200 nM and 300 nM, respectively. Despite the different surface patterns, DII was similar below 200 m at all these stations. Nonetheless, vertical distributions of iodate and iodide had different patterns. From the surface to the Tropical Water at around 150 m, a decrease in iodide concentration was accompanied by an increase of iodate concentration, with a strong gradient between 50 m and 100 m. Below the Tropical Water, both iodide and iodate concentrations are constant. The high concentration of iodide in the surface layer was consistent with that previously reported for the tropical waters. The isopycnals of iodate and iodide in the warm eddy were also depressed in a way similar to salinity, temperature and nutrients.

Discussion

Hydrography and nutrient condition

In the north of SCS, the annual excess precipitation (total precipitation minus evaporation) reaches 1039 mm and most of this precipitation occurs between April and September. The input of fresh water from terrestrial runoffs also occurs mostly in these months. A combination of a generally intense radiative flux together with high rainfall in the north of the SCS induced stratification during the sampling period. The combination of these two fresh water sources reduces the surface salinity in most regions of the central SCS to below 34 [39-41]. Furthermore, the intensive irradiation in tropics induces persistent high SST (Sea-Surface Temperature) in the South China Sea. Thus, the upper water column is always well stratified [41] with the mixed layer shallower than 30 m during most of the year. Meanwhile, the photic zone depth stays constantly at around 85 m throughout the year [26]. The photic zone depth exceeds the mixed layer depth and the top of the nutricline, whereas the mixed layer does not reach the top of the nutricline. Hence, the nutrients in the upper nutricline cannot be made available to fuel photosynthetic activities via vertical mixing [36]. Therefore, the northern South China Sea is oligotrophic during summer and primary production is limited primarily by the availability of the nutrients rather than the availability of light.

Nitrate-salinity and phosphate-salinity graphs are useful in classifying the water column into three distinct biogeochemical regimes, exemplified here by that for nitrate (Figure 8a). The relationship between phosphate and salinity followed the same pattern qualitatively. As shown in Figure 8a, nitrate was almost undetectable in the first 50 m layer where salinity varied between 33.1 and 34.1 (representing by the horizontal limb). Nutrients are imported into the surface layer due to surface cooling and wind-induced vertical mixing in winter, and then depleted by high biological productivities during winter and
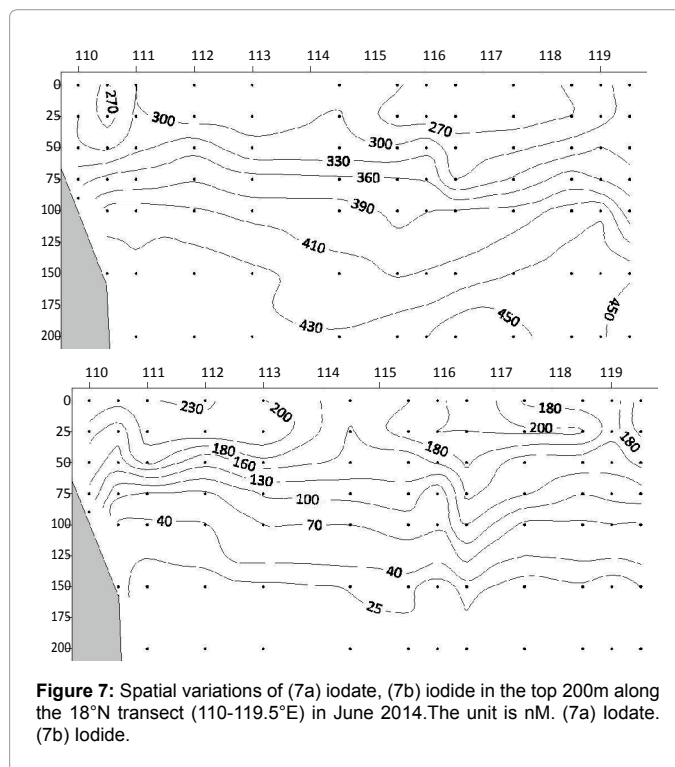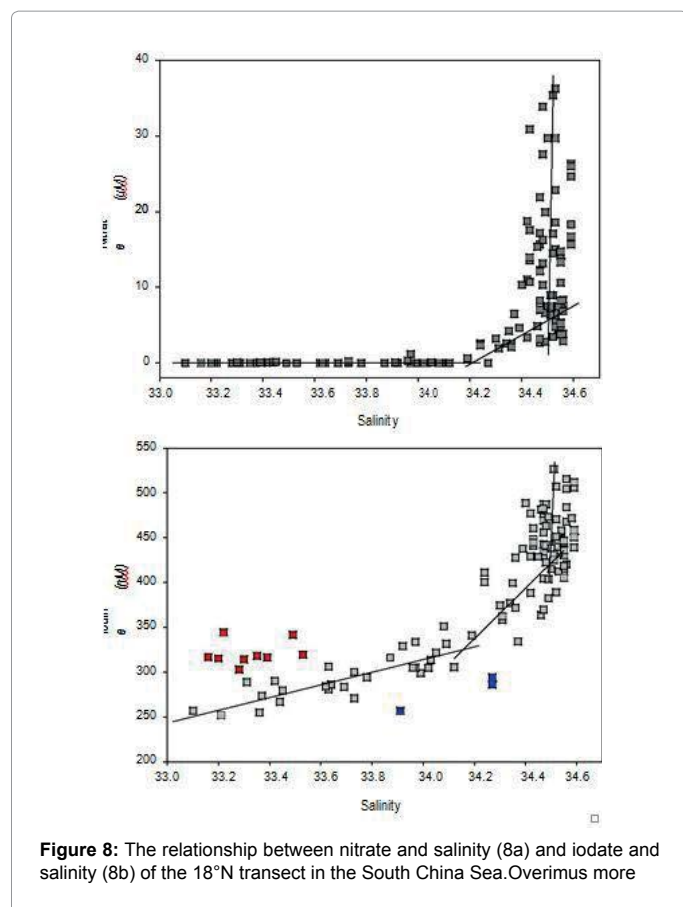

Figure 7: Spatial variations of (7a) iodate, (7b) iodide in the top 200m along the 18°N transect (110-119.5°E) in June 2014.The unit is nM. (7a) Iodate. (7b) Iodide.

Figure 8: The relationship between nitrate and salinity (8a) and iodate and salinity (8b) of the 18°N transect in the South China Sea.Overimus more

spring. Before summer, nutrients were exhausted and photosynthesis was subdued by limited abundance of nutrients, in particular by N. In the layer between the Tropical Water and 1500 m (representing by the nearly vertical line), nitrate increased with depth gradually. The main biogeochemical process here was the re-mineralization of sinking organic matter produced by surface productivity. The gradient of nitrate concentration was higher above 500 m because most of the biologically produced organic matter within the euphotic zone was degraded before falling below 400 m. From 50 m to the layer of the Tropical Water with a salinity maximum at around 150 m (representing by the line connecting the horizontal line and the nearly vertical line), nitrate increased sharply. This layer of rapid nitrate increase layer coincides approximately with the primary nitrite maximum layer. Since nitrate is generated through biologically mediated process of nitrification and nitrite is an intermedium of this process, the nitrite maximum and rapid increase of nitrate between 50 m and 150 m suggest a high activity of nitrifers. Because of intensive nitrification, DO decreases rapidly in this layer.

Dissolved inorganic iodine

As mentioned above, the vertical profiles of Dissolved Inorganic Iodine (DII) can be categorized into two patterns. While stations 2, 6, 7, 10, 11 and 12 had essentially the same concentrations of DII, stations 1, 3, 4, 5, 8, 9 and 13 showed surface enrichments of DII. Apparently, the surface enrichment of DII was interrupted by eddy-induced convection at stations 10, 11, 12 and 6, 7, and by upwelling at station 2. It appears that the surface enrichment of DII is a common phenomenon in the northern South China Sea. The enrichment of total iodine has been

reported in many different environments due to diversified reasons. e.g., in brines such as the Orca Basin [42] and the Mediterranean Sea [43], simultaneous mobilization of chloride and iodide during the dissolution of evaporate beds results in extraordinarily high iodide and total iodine; thin sub-surface maxima of iodide and total iodine found in the pycnocline at 150 m in the Orca Basin [42] and at 100 m in the Venezuela Basin [2] may be resulted from advection or re-mineralization of organic matter forming iodide as the initial product; advection from margin sediments off of India may be the most plausible source of iodine and contributed ~96% of the total excess iodine to the OMZ in the Arabian Sea. Anyhow, these iodine enrichments possessed extraordinarily high iodide concentrations and none of these happened in surface waters. There is only one reported iodine enrichment happened at surface water, i.e., Truesdale et al. [44] observed unusually high iodide concentrations (320-850 nM) in surface waters in the Skagerrak, particularly during the summer cruise. Unfortunately, the cause for such iodine enrichment remained unclear although a surface phenomenon has been speculated. Moreover, this enrichment was also caused by extraordinarily high iodide. In contrast to all these instances enumerated above, the enrichment of iodine within the mixed layer in the northern South China Sea is not so exaggerated and the concentration of iodide still falls within the range of concentrations for surface tropical waters from previous oceanographic measurements. Furthermore, iodate is also slightly higher within the mixed layer at most of these stations showing surface enrichment than the others. Thus, the iodate/iodide ratios of these stations are still similar to those of the other stations.

The surface waters in the SCS exchange freely with those in the East China Sea, the Java Sea, the Sulu Sea and the western Philippine Sea. In addition, a multitude of rivers drain into the South China Sea after they have passed through densely populated areas. External import of sources with elevated iodine from these areas and relatively longer residence time of the mixed layer may cause enrichment of DII in the northern South China Sea. Atmospheric deposition may be another potential source of excess total iodine to the mixed layer.

Interconversion of iodide and iodate

A close examination of data in Figure 5a and 5b reveals that the vertical distribution of iodate resembles that of nitrate (also phosphate, not shown). Relationships between iodate and nitrate/phosphate show a strong positive correlation, yielding 0.9 and 0.8 respectively. As for nitrate, we use the iodate-salinity graph to classify different biogeochemical regimes of iodine (Figure 8b). The iodide-salinity graph is symmetrically reversed to iodate-salinity graph.

The similarity between the iodate-salinity graph and the nitrate-salinity graph indicates strong coupling of iodine speciation and nutrients. In the upper 50 m layer (salinity between 33.10 and 34.12), iodate is proportionally depleted and nitrate is almost undetectable respectively. In this photic layer, iodate reduction dominates and iodide should be the main product of iodate reduction since iodide accounts for ~40% of DII here. Although we did not measure organic iodine, the organic iodine may also be produced. Iodate reduction might depend upon biotic processes including phytoplankton [7,16,45,46] and bacterial action during respiration [9,47], and abiotic processes including photochemical reduction initiated by organic matter [48] and reaction with sulfide [14]. Since the photochemical reduction of iodate by iodide at natural concentrations in seawater cannot account for the extent of iodate reduction in surface seawaters [49] and chemical redox reactions are not possible to occur in open oceanic environment, the formation of iodide here must be caused mainly by biological activities

in surface waters of the northern South China Sea. While nutrients were already exhausted by biological activities and photosynthesis was low in the summer, the large percent of iodide may be produced by high phytoplanktonic productivity during winter and spring and intense bacterial action. The red points above the line indicated relatively high iodate concentrations and enrichment of DII in the mixed layer. The blue points indicated lower iodate concentrations on the continental shelf. Meanwhile, the DII of these three blue points were lower than the ambient waters, possibly indicating the formation of organic iodine.

In the layer between the Tropical Water and 1500 m (representing by the vertical line in Figure 8b), iodate increases with depth slightly from 150 m to 200 m and then becomes almost invariant with several higher concentration points. While a large percent of iodate was reduced to iodide at the surface, it became the predominant species of iodine below the Tropical Water. Meanwhile, nitrate increases gradually in this thick layer due to re-mineralization of sinking particles. As compared with nitrate, very little iodine is turned into particulate form through biological activities. Meanwhile, most of the biologically produced organic matter within the euphotic zone was degraded before it reached 400 m. Thus iodate stayed quite constant while nitrate increased gradually through the water column to 1500 m.

From 50 m to the depth of the Tropical Water, iodate increases while iodide decreases. Relative to the surface 50 m layer, this layer of water has high concentration of macro-nutrients. Furthermore there is a subsurface chlorophyll maximum [50].

But iodide formation was lower in despite of higher phytoplanktonic activities. Thus, the opposite process should dominate. Song et al. [51] found that bacteria played an important role in the oligotrophic waters of the South China Sea and bacterial production was closely correlated to the phytoplankton biomass and primary production, and maximum bacterial production occurs near bottom layers of the euphotic zone. Combining with their findings, the nitrite maximum and rapid increase of nitrate between 50 m and the Tropical Water at around 150 m suggest high activity of nitrifers, i.e., strong nitrification. On the other hand, iodide oxidation may occur in parallel with bacterial nitrification at the base of the photic zone in the northern South China Sea. The "nitrification hypothesis" was proposed by Truesdale et al. [52] who apply a box model to the Black Sea and the hypothesis is supported by direct observations of iodide oxidation and iodate formation in anchialine systems [23,47,53]. In the global biogeochemical model of nitrification proposed by Yool et al. [54], for much of the world ocean a substantial fraction of the nitrate that is taken up biologically is generated through recent nitrification near the surface [55]. At the global scale, nitrification accounts for about half of the nitrate consumed by growing phytoplankton [56]. Based on strong nitrification, the extent of iodide oxidation in parallel with nitrification may be presumed to be sufficient to compete with iodide formation at the base of the photic zone and thus iodide was reduced quickly.

Conclusions

Vertical distributions of iodate and iodide have different patterns. Above the Tropical Water at around 150 m, iodide concentration decreased while iodate concentration increased. Below the Tropical Water, both iodide and iodate are constant. Iodide concentrations were high at the surface mixed layer but fall within the range of concentrations previously reported for surface tropical waters. The speciation of iodine was strongly influenced by biological activities such as photosynthesis and bacterial action in the South China Sea. Thus, iodine speciation is coupled with nutrients. In the mesoscale warm eddy, the isopycnals

of hydrographic factors (salinity, temperature), dissolved oxygen, nutrients and iodine species were depressed due to downwelling. This work is a preliminary survey of the dissolved inorganic iodine in the northern South China Sea. Further investigations are needed to better understand the biogeochemistry of iodine in this typical marginal sea.

References

1. Leblanc C, Colin C, Cosse A, Delage L, La Barre S, et al. (2006) Iodine transfers in the coastal marine environment: the key role of brown algae and of their vanadium-dependent haloperoxidases. Biochimie 88: 1773-1785.

2. Wong GTF, Brewer PG (1977) The marine chemistry of iodine in anoxic basins. Geochimica et Cosmochimica Acta 41: 151-159.

3. Wong GTF (1980) The stability of dissolved inorganic species of iodine in seawater. Marine Chemistry 9: 13-24.

4. Wong GTF (1991) The marine geochemistry of iodine. Reviews in Aquatic Sciences 4: 45-73.

5. Tsunogai S, Henmi T (1971) Iodine in the surface water of the ocean. Journal of Oceanographical Society of Japan 27: 67-72.

6. Elderfield H, Truesdale VW (1980) On the biophilic nature of iodine in seawater. Earth and Planetary Science Letters 50: 105-114.

7. Campos M, Farrenkopf AM, Jickells TD, Luther GW (1996) A comparison of dissolved iodine cycling at the Bermuda Atlantic Time-Series station and Hawaii Ocean Time-Series Station. Deep-Sea Research Part II: Topical Studies in Oceanography 43: 455-466.

8. Farrenkopf AM, Luther Ш GW (2002) Iodine chemistry reflects productivity and denitrification in the Arabian Sea: evidence for flux of dissolved species from sediments of western India into the OMZ. Deep Sea Research Part II: Topical Studies in Oceanography 49: 2303-2318.

9. Truesdale VW, Bailey GW (2002) Iodine distribution in the Southern Benguela system during an upwelling episode. Continental Shelf Research 22: 39-49.

10. Wong GTF, Zhang LS (1992a) Changes in iodine speciation across coastal hydrographic fronts in southeastern United States continental shelf waters. Continental Shelf Research 12: 717-733.

11. Truesdale VW (1994) A re-assessment of redfield correlations between dissolved iodine and nutrients in oceanic waters and a strategy for further investigations of iodine. Marine Chemistry 48: 43-56.

12. Truesdale VW, Bailey GW (2000) Dissolved Iodate and Total Iodine during an Extreme Hypoxic Event in the Southern Benguela System. Estuarine, Coastal and Shelf Science 50: 751-760.

13. Truesdale VW, Jones K (2000) Steady-state mixing of iodine in shelf seas off the British Isles. Continental Shelf Research 20: 1889-1905.

14. Truesdale VW, Upstill-Goddard R (2003) Dissolved iodate and total iodine along the British east coast. Estuarine, Coastal and Shelf Science 56: 261-270.

15. Truesdale VW, Bale AJ, Woodward EMS (2000) The meridional distribution of dissolved iodine in near-surface waters of the Atlantic Ocean. Progress In Oceanography 45: 387-400.

16. Wong GTF, Zhang LS (2003) Seasonal variations in the speciation of dissolved iodine in the Chesapeake Bay. Estuarine, Coastal and Shelf Science 56: 1093-1106.

17. Chance R, Malin G, Jickells TD, Baker AR (2007) Reduction of iodate to iodide by cold water diatom cultures. Marine Chemistry 105: 169-180.

18. Von Glasow R. (2005) Seaweed, Iodine, New Particles and Atmospheric Chemistry-The Current State of Play. Environmental Chemistry 2: 243.

19. Bluhm K, Croot P, Huhn O, Rohardt G, Lochte K (2011) Distribution of iodide and iodate in the Atlantic sector of the southern ocean during austral summer.

Deep Sea Research II: Topical Studies in Oceanography 58: 2733-2748.

20. Truesdale VW, Nausch G, Baker A (2001a) The distribution of iodine in the Baltic Sea during summer. Marine Chemistry 74: 87-98.

21. Waite TJ, Truesdale VW, Olafsson J (2006) The distribution of dissolved inorganic iodine in the seas around Iceland. Marine Chemistry 101: 54-67.

22. Chance R, Weston K, Baker AR, Hughes C, Malin G, et al. (2010) Seasonal and interannual variation of dissolved iodine speciation at a coastal Antarctic site. Marine Chemistry 118: 171-181.

23. Zic V, Caric M, Viollier E, Ciglenecki I (2010) Intensive sampling of iodine and nutrient speciation in naturally eutrophicated anchialine pond (Rogoznica Lake) during spring and summer seasons. Estuarine, Coastal and Shelf Science 87: 265-274.

24. Chen CTA, Wang SL, Wang BJ, Pai SC (2001) Nutrient budgets for the South China Sea basin. Marine Chemistry 75: 281-300.

25. Cai SQ, Su JL, Gan ZJ, Liu Q (2002) The numerical study of the South China Sea upper circulation characteristics and its dynamic mechanism, in winter. Continental Shelf Research 22: 2247-2264.

26. Tseng CM, Wong GTF, Lin I.I., Wu CR, Liu KK (2005) A unique seasonal pattern in phytoplankton biomass in low-latitude waters in the South China Sea. Geophysical Research Letters 32: 4.

27. Yuan YC, Liao GH, Yang CH (2009) A diagnostic calculation of the circulation in the upper and middle layers of the Luzon Strait and the northern South China Sea during March 1992. Dynamics of Atmospheres and Oceans 47: 86-113.

28. Morton B, Blackmore G (2001) South China Sea. Marine Pollution Bulletin 42: 1236-1263.

29. Gan JP, Li L, Wang DX, Guo XG (2009) Interaction of a river plume with coastal upwelling in the northeastern South China Sea. Continental Shelf Research 29: 728-740.

30. Su JL (2004) Overview of the South China Sea circulation and its influence on the coastal physical oceanography outside the Pearl River Estuary. Continental Shelf Research 24: 1745-1760.

31. Jing ZY, Qi YQ, Hua ZL, Zhang H (2009) Numerical study on the summer upwelling system in the northern continental shelf of the South China Sea. Continental Shelf Research 29: 467-478.

32. Strickland JDH, Parsons TR (1972) A Practical Handbook of Seawater Analysis, Bulletin 167, second ed. Fisheries Research Board of Canada, Ottawa.

33. Wong GTF, Zhang LS (1992b) Chemical removal of oxygen with sulfite for the polarographic or voltammetric determination of iodate or iodide in seawater. Marine Chemistry 38: 109-116.

34. Herring JR, Liss PS (1974) A new method for the determination of iodine species in seawater. Deep Sea Research and Oceanographic Abstracts 21: 777-783.

35. Luther Ш GW, Swartz CB, Ullman WJ (1988) Direct determination of iodide in seawater by cathodic stripping square wave voltammetry. Analitical Chemistry 60: 1721-1724.

36. Wong GTF, Tseng CM, Wen LS, Chung SW (2007) Nutrient dynamics and N-anomaly at the SEATS station. Deep Sea Research Part II: Topical Studies in Oceanography 54: 1528-1545.

37. Codispoti LA, Christensen JP (1985) Nitrification, denitrification and nitrous oxide cycling in the Eastern Tropical South Pacific Ocean. Marine Chemistry 16: 277-300.

38. Ward BB (1987) Nitrogen transformation in the Southern California bight. Deep-Sea Research 34: 785-805.

39. Gong GC, Liu KK, Liu CT, Pai SC (1992) The chemical hydrography of the South China Sea west of Luzon and a comparison with the West Philippine Sea. Terrestrial, Atmospheric and Oceanic Sciences 3: 587-602.

40. Shaw PT (1991) The seasonal variation of the intrusion of the Philippine Sea water into the South China Sea. Journal of Geophysical Research 96: 821-827.

41. Shaw PT, Chao SY (1994) Surface circulation in the South China Sea. Deep Sea Research Part I: Oceanographic Research Papers 41: 1663-1683.

42. Wong GTF, Takayanagi K, Todd JF (1985) Dissolved iodine in waters overlying and in the Orca Basin, Gulf of Mexico. Marine Chemistry 17: 177-183.

43. Ullman WJ, Luther GW, De Lange GJ, Woittiez JR (1990) Iodine chemistry in deep anoxic basins and overlying waters of the Mediterranean Sea. Marine Chemistry 31: 153-170.

44. Truesdale VW, Danielssen DS, Waite TJ (2003) Summer and winter distributions of dissolved iodine in the Skagerrak. Estuarine, Coastal and Shelf Science 57: 701-713.

45. Moisan TA, Dunstan WM, Udomkit A, Wong GTF (1994) The uptake of iodate by marine phytoplankton. Journal of Phycology 30: 580-587.

46. Tian RC, Marty JC, Nicolas E, Chiavérini J, Ruiz-Ping D, et al. (1996) Iodine speciation: a potential indicator to evaluate new production versus regenerated production. Deep Sea Research Part I: Oceanographic Research Papers 43: 723-738.

47. ZicV, Truesdale VW, Cukrov N (2008) The distribution of iodide and iodate in anchialine cave waters --Evidence for sustained localised oxidation of iodide to iodate in marine water. Marine Chemistry 112: 168-178.

48. Spokes LJ, Liss PS (1996) Photochemically induced redox reactions in seawater, II. Nitrogen and iodine. Marine Chemistry 54: 1-10.

49. Truesdale VW (2007) On the feasibility of some photochemical reactions of iodide in seawater. Marine Chemistry 104: 266-281.

50. Lu ZM, Gan JP, Dai MH, Cheung AYY (2010) The influence of coastal upwelling and a river plume on the subsurface chlorophyll maximum over the shelf of the northeastern South China Sea. Journal of Marine Systems 82: 35-46.

51. Song XY, Liu HX, Huang LM, Tan YH, Ke ZX, et al. (2010) Distribution characteristics of basic biological production and its influencing factors in the northern South China Sea in summer. Acta Ecologica Sinica 30: 6409-6417.

52. Truesdale VW, Watts SF, Rendell AR (2001b) On the possibility of iodide oxidation in the near-surface of the Black Sea and its implications to iodine in the general ocean. Deep-Sea Research Part I: Oceanographic Research Papers 48: 2397-2412.

53. Zic V, Branica M (2006) The distributions of iodate and iodide in Rogoznica Lake (East Adriatic Coast). Estuarine Coastal and Shelf Science 66: 55-66.

54. Yool A, Martin AP, Fernandez C, Clark DR (2007) The significance of nitrification for oceanic new production. Nature 447: 999-1002.

55. Karl DM, Lukas R (1996) The Hawaii Ocean Time-series (HOT) program: background, rationale and field implementation. Deep-Sea Research Part II: Topical Studies in Oceanography 43: 129-156.

56. Wyrtki K (1961) Scientific Results of Marine Investigations of the South China Sea and the Gulf of Thailand. Physical oceanography of the Southeast Asian waters 2: 195.